Development 137, 4005-4015 (2010) doi:10.1242/dev.053173

Characterisation of a new regulator of BDNF signalling, Sprouty3, involved in axonal morphogenesis in vivo

Niki Panagiotaki[1], Federico Dajas-Bailador[1], Enrique Amaya[1,2,*,†], Nancy Papalopulu[1,*,†] and Karel Dorey[1,2,*,†]

SUMMARY

During development, many organs, including the kidney, lung and mammary gland, need to branch in a regulated manner to be functional. Multicellular branching involves changes in cell shape, proliferation and migration. Axonal branching, however, is a unicellular process that is mediated by changes in cell shape alone and as such appears very different to multicellular branching. Sprouty (Spry) family members are well-characterised negative regulators of Receptor tyrosine kinase (RTK) signalling. Knockout of *Spry1*, *2* and *4* in mouse result in branching defects in different organs, indicating an important role of RTK signalling in controlling branching pattern. We report here that Spry3, a previously uncharacterised member of the Spry family plays a role in axonal branching. We found that *spry3* is expressed specifically in the trigeminal nerve and in spinal motor and sensory neurons in a Brain-derived neurotrophin factor (BDNF)-dependent manner. Knockdown of Spry3 expression causes an excess of axonal branching in spinal cord motoneurons in vivo. Furthermore, Spry3 inhibits the ability of BDNF to induce filopodia in *Xenopus* spinal cord neurons. Biochemically, we show that Spry3 represses calcium release downstream of BDNF signalling. Altogether, we have found that Spry3 plays an important role in the regulation of axonal branching of motoneurons in vivo, raising the possibility of unexpected conservation in the involvement of intracellular regulators of RTK signalling in multicellular and unicellular branching.

KEY WORDS: BDNF, Sprouty, TrkB, *Xenopus*, Branching, Motoneuron

INTRODUCTION

The establishment of correct neuronal connections, also known as neuronal wiring, is crucial for the function of the nervous system in vertebrates. Axons have to navigate through their environment and interpret extracellular cues in order to find their target cells and make synaptic connections (O'Donnell et al., 2009). Axon branching allows neurons to establish multiple connections with their target cells, which can be neuronal or non-neuronal. Therefore, axon branching is an essential process for neuronal wiring during the development, repair and plasticity of the nervous system (Acebes and Ferrus, 2000; Navarro, 2009). Numerous studies have explored the role of extrinsic cues (including netrins, semaphorins and neurotrophins) in the control of neuronal branching (Campbell et al., 2001; Feldner et al., 2007; Marler et al., 2008; Morita et al., 2006; Tang et al., 2004). By contrast, relatively little is known about the role of intrinsic mechanisms that regulate axonal branching (Goldberg, 2004).

Brain-derived neurotrophic factor (BDNF) is a signalling molecule involved in multiple aspects of neural development (Reichardt, 2006). BDNF belongs to the neurotrophin family of extracellular ligands, together with Neurotrophin 3 and 4 (NT3 and NT4) and Nerve growth factor (NGF). Neurotrophins are secreted as pro-proteins and undergo further maturation in the extracellular space (Reichardt, 2006). Whereas pro-neurotrophins have high affinity for the p75NTR receptor (a member of the tumor necrosis factor family), the mature forms of neurotrophins bind the Receptor tyrosine kinase (RTK) of the Trk subfamily with high affinity. BDNF binds specifically to TrkB, inducing TrkB dimerisation and activation of its kinase activity by trans-autophosphorylation (Cunningham and Greene, 1998). Subsequently, TrkB can activate various intracellular pathways, such as the Erk, the PI3K-Akt and the PLCγ-Ca^{2+} pathways (Segal, 2003). The BDNF-TrkB pathway regulates a variety of cellular responses, including the differentiation and survival of different types of neurons (Barde et al., 1982; Huang and Reichardt, 2001; Xu et al., 2000), axonal branching and arborisation of specific neuronal subtypes (Cohen-Cory and Fraser, 1995; Huang et al., 2007), as well as neurite and dendrite outgrowth (Huang and Reichardt, 2001; Xu et al., 2000). Furthermore, BDNF acts as a guidance cue (Ming et al., 1997; Ming et al., 1999), modulates synaptic plasticity (Yoshii and Constantine-Paton, 2010) and plays an important role in long-term memory (Minichiello, 2009). How a single signalling pathway can control so many biological processes is still poorly understood, but it is likely to involve numerous positive- and negative-feedback loops that allow the cell to interpret correctly the signal it receives.

The Sprouty (Spry) proteins form a family of intracellular negative regulators of RTK signalling. Spry was first identified as a negative regulator of FGF signalling in the *Drosophila* trachea (Hacohen et al., 1998). Loss-of-function of Spry in *Drosophila* leads to excess branching of the tracheal system, a phenotype that resembles an FGF gain-of-function phenotype (Hacohen et al., 1998). Subsequently, four Spry family members (Spry1, 2, 3 and 4) have been identified in vertebrates (Mason et al., 2006). They all share a conserved cysteine-rich domain, the spry domain, and a conserved tyrosine residue in the N-terminus (Kim and Bar-Sagi, 2004). Knockout studies have shown that Spry1, 2 and 4 are involved in numerous developmental processes. The phenotype of the different knockouts is always associated with an excess of RTK

[1]Faculty of Life Sciences, Michael Smith Building, University of Manchester, Oxford Road, Manchester, M13 9PT, UK. [2]The Healing Foundation Centre, Michael Smith Building, University of Manchester, Oxford Road, Manchester, M13 9PT, UK.

*These authors contributed equally to this work
†Authors for correspondence (enrique.amaya@manchester.ac.uk; nancy.papalopulu@manchester.ac.uk; karel.dorey@manchester.ac.uk)

Accepted 21 September 2010

signalling (Furthauer et al., 2001; Klein et al., 2006; Shim et al., 2005; Taniguchi et al., 2007; Taniguchi et al., 2009a; Taniguchi et al., 2009b). Interestingly, downregulation or overexpression of different Spry family members often results in branching defects in different organs. For example, *Spry1* knockout causes an increase in ureteric buds in the kidney (Basson et al., 2005; Basson et al., 2006). *Spry4* knockout results in increased branching of peripheral blood vessels of the vascular system, probably because of excessive VEGF signalling (Taniguchi et al., 2009b). Knockdown of Spry2 expression in murine embryonic lung cells in culture enhances branching morphogenesis (Tefft et al., 1999). In PC12 cells and cerebellar granule neurons (CGNs), overexpression of Spry2 reduces the number of neurites (Gross et al., 2007; Hanafusa et al., 2002; Sasaki et al., 2001). However, there is still a lack of evidence to support a role for Spry in axonal branching, as none of the knockouts reported to date shows a defect in the central nervous system. This could be due to some level of redundancy between Spry family members or because another Spry family member might have a role in neuronal branching in vivo.

We report here the role of a previously uncharacterised member of the Spry family, Spry3, during axonal branching morphogenesis. *spry3* expression in *Xenopus* embryos is restricted to the trigeminal nerve and to both sensory and motor neurons in the spinal cord and is dependent on BDNF-TrkB signalling. Loss-of-function experiments in *Xenopus* embryos show that Spry3 specifically represses the formation of new branches in motoneurons. In *Xenopus* spinal cord neurons in culture, loss of Spry3 expression causes an excess of axonal filopodia in a BDNF signalling-dependent manner. Furthermore, in mouse cortical neurons, Spry3 overexpression reduces the number of branches induced by BDNF, indicating that Spry3 function might be conserved in mammals. Finally, Spry3 specifically regulates the Ca^{2+} pathway downstream of BDNF-TrkB signalling. Altogether, we show that Spry3 is a novel regulator of axonal branching during embryonic development and a negative regulator of calcium signalling downstream of BDNF-TrkB.

MATERIALS AND METHODS

Isolation of *spry3* and other constructs

X. tropicalis (*Xt*) *spry3* and *spry4* were cloned by PCR using genomic DNA, and *X. tropicalis trkb* using pCMV SPORT6 Trkb as a template with the following oligonucleotides (5′ to 3′): *spry3* fwd GGGAATTCATGGATATTTCAACTGCAGATATCC and rev GGCTCGAGTCATACAGGCTTATCAAAAGGCC; *spry4* fwd CGGAATTCATGGATTCCAGGATTCC and rev GGCTCGAGTCAGAATGGCTTCTCTGG; *trkb* fwd GAATTCATGCGCCTCTGGAAAGGCTCC and rev CTCGAGTTAGCCAAGGATATCAAGGTATAC. In all cases, the amplified fragment was cloned into pCS2 using *Eco*RI and *Xho*I (underlined sequences). To generate HA-tagged constructs, Spry2, Spred1 (Sivak et al., 2005) and Spry3 were subcloned into pFtx11. *bdnf* was cloned into pCR4.1 after amplification using primers fwd 5′-GAATTCATGACCATCCTTTTCCTTACTATG-3′ and rev 5′-CTCGAGCTATCTTCCCCTTTTAATGGTC-3′. All constructs were verified by sequencing. For in situ hybridisation, the following constructs were used: pCS107 Hox11L2 (clone TTpA003i09), pCS107 HB9 (clone THdA004g15), pCR2.1 5′UTR Spry3, pCR4 Xt BDNF, pCMV SPORT6 Xt TrkB (IMAGE: 7655094), pCS2 Xt Spry4 and pCS107 Xt fgf8b (Lea et al., 2009). For transfection, the following constructs were used: pCS2 GFP, pCS2 Xt Spry3 and pCS2 Xt TrkB.

Morpholinos, microinjections and inhibitor treatment

The following morpholinos (Gene Tools) were used (5′ to 3′): MO spry3 e1i1 AAGAAGACTCACCTCTGTAAGACTG; MO spry3 i1e2 CTGATGATCCTGCACAATGAGAATA; and MO TrkB CCAGAGGCGCATGGTGGATCTCCGG. MO BDNF and MO control (MOC) were described previously (Huang et al., 2007). All morpholinos were injected at the 1-cell stage as 17 ng MOS3 (8.5 ng of MO spry3 e1i1 plus 8.5 ng of MO spry3 i1e2), 17 ng MO TrkB and 8.5 ng MO BDNF.

Synthetic mRNA was generated using the Ambion mMessenger Kit according to the manufacturer's instructions. For the animal cap assay, 0.5 ng *trkb*, 1 ng *spred1*, 0.1 ng *spry2* and 0.4 ng *spry3* were injected.

For the inhibition of FGFR, the small chemical inhibitor SU5402 (Calbiochem) was used as previously described (Sivak et al., 2005). The TrkB inhibitor K252a (Calbiochem) was used at 1 μM. The PLCγ inhibitor U73122 (Calbiochem) was used at 10 and 50 μM final concentration.

Cell culture

Spinal cords of stage 20 *Xenopus tropicalis* embryos were dissected in a Ca^{2+}- and Mg^{2+}-free solution (115 mM NaCl, 2.5 mM KCl, 10 mM Hepes, 0.5 mM EDTA, pH 7.4). The dissociated spinal neurons and myocytes were transferred into a 50-mm glass-bottom dish (MatTek) coated with 10 μg/ml poly-L-lysine and 10 μg/ml laminin. The cells were cultured in 50% Ringer's Solution (115 mM NaCl, 2 mM $CaCl_2$, 2.5 mM KCl, 10 mM Hepes, pH 7.4) plus 49% Leibovitz-15 medium (Sigma) and 1% penicillin/streptomycin (Cambrex). The neuron-myocyte cultures were incubated at 23°C for 24 hours before live imaging (Gomez et al., 2003).

Mouse cortical neurons from embryonic day (E) 16 were isolated and transfected as previously described (Dajas-Bailador et al., 2008) with 2 μg Spry3 DNA + GFP DNA or 2 μg GFP DNA alone as a control. On day 5, the GFP-positive neurons were assessed for the number of branches projecting from the axon. Cortical neurons stimulated with BDNF were treated at two 24-hour intervals with 100 ng/ml BDNF.

HeLa cells were cultured in DMEM supplemented with 10% fetal calf serum and antibiotics. Individual plasmid DNA constructs were transfected into 60% confluent cells by lipofection (using Lipofectamine 2000, Invitrogen) following the manufacturer's instructions. A total of 1.6 μg DNA was transfected per well in a 12-well plate. After 8 hours, the medium was changed to DMEM containing 0.5% serum and incubation continued overnight. The cells were then treated with 100 ng/ml recombinant BDNF for the indicated time before being lysed in Lysis Buffer (150 mM NaCl, 50 mM Tris pH 7.5, 1 mM EDTA/EGTA, 0.5% NP40).

Isolation of RNA and RT-PCR

Total RNA from whole embryos or spinal cord neurons in culture was isolated using Trizol (Invitrogen) according to the manufacturer's instructions. cDNA was generated using SuperScript II reverse transcriptase (Invitrogen) and the PCR was performed using Taq polymerase (Roche) with the following oligonucleotides (5′ to 3′): *spry3* fwd TGCTAAGGCAGAGCCACTCTGTC and rev CACCAAATGATCATGAGGCCACTC; *spry4* fwd GTCACTCATTCGCTGGGATTTGC and rev GATGAGCGTGGGTTCATGAGG; *bdnf* fwd CCGAAGACCAAGCCTGAATA and rev GAGTACCATGGGTCCGAAGA; *trkb* fwd CCTACTTGCCTTGGTTTGGA and rev CTGGAAAGGATTGCCACCTA. Oligonucleotides for *spry1*, *spry2* (Sivak et al., 2005) *odc* (Heasman et al., 2000) and β-*globin* (Costa et al., 2008) are described elsewhere.

For real-time PCR, the data for each sample were normalised to the expression level of *ribosomal protein L8* (*rpl8*) and calculated by the $2^{-\Delta Ct}$ method (Chen et al., 2009). Real-time RT-PCR analysis was performed using a Chromo4 Real-Time PCR Detector (Bio-Rad). *spry3* oligonucleotides were fwd 5′-GGGATTATACTCATTTAAAGCACCATGGAT-3′ and rev 5′-TGGTATGGTCCATCAAGGTACATCT-3′; the internal FAM-labelled probe was 5′-CAGTCTTACAGAGGATCATC-3′ (a generous gift from ABI).

Immunoblotting and $^{45}Ca^{2+}$ efflux assay

The equivalent of ten animal caps, one total embryo or 50 μg HeLa cell extract was loaded on SDS-PAGE. The proteins were transferred to a PDVF membrane and stained with the following primary antibodies: anti-pErk (Sigma, clone YT; 1:10,000), anti-Erk (Cell Signaling; 1:1000), anti-pAkt (Cell Signaling; 1:1000), anti-Akt (Cell Signaling; 1:1000) and custom anti-Spry3. In all cases, HRP-coupled secondary antibodies (Dako) and the ECL (Pierce) chemiluminescence detection method were used.

Oocytes were isolated and injected with 0.5 ng of *trkb* and 5 ng of *spred1*, *spry2*, *spry3* or GFP mRNA. After 48 hours in culture in modified Barth's saline (MBSH) at 16°C, Ca^{2+}-efflux assays were performed as described previously (Musci et al., 1990).

In situ hybridisation, immunofluorescence and imaging

Whole-mount in situ hybridisations and sections were performed essentially as previously described (Harland, 1991; Lea et al., 2009). Whole-mount immunofluorescence and imaging were performed as described (Huang et al., 2007) using the following primary antibodies: mouse anti-acetylated α-tubulin (Sigma), mouse anti-12/101 (Developmental Studies Hybridoma Bank) and rabbit anti-GFP (Abcam). For sectioning, whole-mount stained embryos were incubated in an acrylamide mixture, consisting of 2.4 ml 40% acrylamide, 0.3 ml 10× PBS and 0.3 ml 2% ammonium persulphate, for 1 to 3 hours and the acrylamide mixture solidified by adding Temed. The blocks were sectioned using a vibratome at 70 μm, perpendicular to the orientation of the embryo. The sections were mounted in Mowiol (Polysciences). Motor axonal tracts on acrylamide sections were imaged using an Olympus Fluoview FV1000 confocal microscope. For each embryo, branch points were quantified from eight sections using Imaris software (Bitplane).

For live differential interference contrast (DIC) imaging of spinal cord neurons, an inverted Nikon Eclipse TE2000-E microscope was used. DIC images were taken at a standard rate of one frame every 30 seconds. The neurons were imaged in the culture medium, and at 20 minutes 100 ng/ml BDNF (R&D Systems) was added into the medium. Imaging was continued for another 30 minutes. The images were processed using ImageJ (http://rsb.info.nih.gov/ij) to generate time-lapse movies. Quantitative analysis of the number of filopodia projecting from the neurons was performed manually at a rate of one frame per minute.

Statistical analysis

In all cases, the normal distribution of the dataset was verified before applying Student's *t*-test (paired or unpaired, as indicated in the figure legend). All tests were two-tailed and the alpha power was always greater than 0.8. The statistical analyses were performed using SigmaStat (v3.0) (Systat Software).

RESULTS

Identification of *Xenopus* Spry3

To identify *Xenopus tropicalis spry3*, we used the mouse *Spry3* sequence to blast *Xenopus tropicalis* ESTs. This led to the identification of a partial EST (DT533112.1) encompassing the 5′UTR and part of the coding sequence. Given that all *spry* genes studied so far contain a single coding exon, we used the partial EST to blast the *Xenopus tropicalis* genome and determined the full coding sequence of *Xenopus* Spry3 (GenBank accession number GU180240, ref. seq. NM_001170509). We subsequently constructed a phylogram tree of the protein sequences of Spry family members from *Xenopus*, mouse and zebrafish using ClustalW2 (http://www.ebi.ac.uk/Tools/clustalw2/index.html) to confirm that the sequence we identified is that of the *Xenopus* orthologue of Spry3 (Fig. 1A). Comparison of Spry3 protein sequence from mouse, *Xenopus* and zebrafish (Fig. 1B) shows that Spry3 exhibits 54.6% homology between the *Xenopus* and zebrafish sequences, 58.7% homology between the *Xenopus* and mouse sequences and 53% homology between the zebrafish and mouse sequences. The homology is higher in the conserved cysteine-rich C-terminal spry domain, where *Xenopus* and zebrafish share 66.4% similarity, *Xenopus* and mouse share 72.7% similarity and zebrafish and mouse 65% similarity.

Characterisation of *spry3* expression in *Xenopus*

To investigate the role of Spry3 during development, we first compared the temporal pattern of expression of the four *Xenopus spry* genes by RT-PCR. As we previously reported, expression of *spry1* and *spry2* peaks at gastrulation (stage 10 and 10.5, Fig. 2A) (Sivak et al., 2005). Whereas *spry2* expression remained at a low level after gastrulation, *spry1* expression peaked again at stages 19-23. By contrast, *spry3* was first expressed at stage 12.5, and its expression increased as development proceeded. *Spry4* was expressed at low levels during gastrulation and then its expression steadily increased (Fig. 2A).

We then investigated the spatial pattern of expression of the four *spry* family members in stage 28 *Xenopus* embryos. *spry1*, *spry2* and *spry4* had a very similar pattern of expression. They were expressed in the forebrain, midbrain-hindbrain boundary, branchial arches and the tailbud (Fig. 2B). However, *spry3* was expressed specifically in the spinal cord and the trigeminal nerve (Fig. 2B). We then performed a more detailed analysis of *spry3* expression during *Xenopus* development (Fig. 2C). We could not detect any *spry3* transcript at gastrula stage, in agreement with our RT-PCR data. At early neurula stage (stage 15), *spry3* was expressed at low

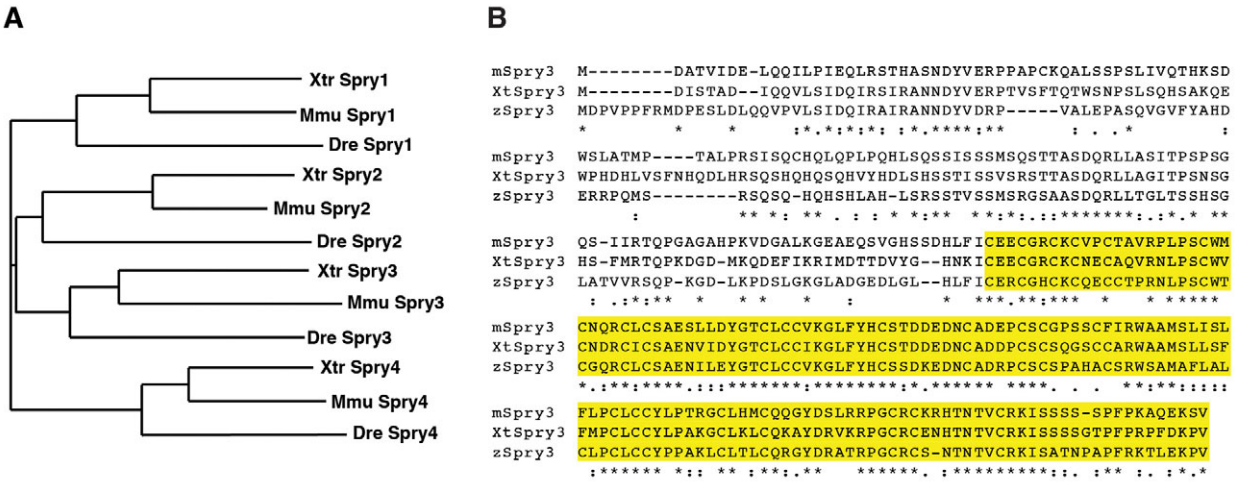

Fig. 1. Characterisation of Spry3 sequence. (**A**) Phylogram tree of the Spry family members from *Xenopus* (*Xenopus tropicalis*, *Xtr*), mouse (*Mus musculus*, *Mmu*) and zebrafish (*Danio rerio*, *Dre*) using ClustalW2. (**B**) Alignment of the Spry3 protein sequences from *Xenopus* (Xt), mouse (m) and zebrafish (z). Asterisk, identical residues; colon, conserved residues; dot, semi-conserved residues. The conserved Spry domain is highlighted in yellow.

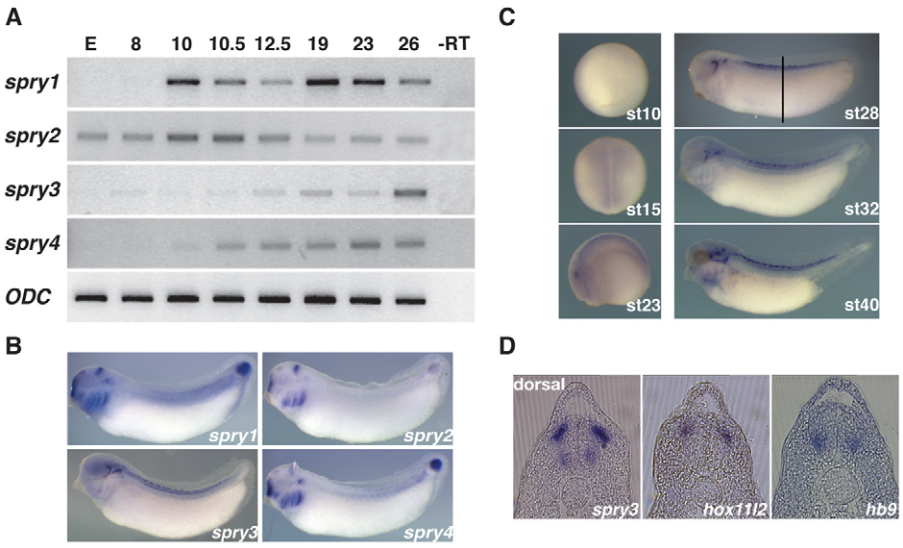

Fig. 2. Temporal and spatial expression pattern of *spry3*. (**A**) Total RNA was isolated from *Xenopus* of the indicated stages and RT-PCR performed using oligonucleotides specific for the indicated genes. E, embryo; –RT, stage 26 without reverse transcriptase. *odc* is a loading control. (**B**) Comparison of the pattern of expression of *spry1*, *spry2*, *spry3* and *spry4* at stage 32. (**C**) Analysis of the spatial expression of *spry3* during *Xenopus* development. Embryos at the indicated stages were fixed and subjected to whole-mount in situ hybridisation using a probe specific for *spry3*. (**D**) Sections (plane indicated in C) of embryos stained with the indicated probes, showing expression in differentiated motor and sensory neurons.

levels in the neural plate, whereas its expression was restricted to the trigeminal nerve and spinal cord after neural tube closure (stages 23-45, Fig. 2C). To investigate further the expression pattern of *spry3* in the spinal cord, stage 28 embryos stained for *spry3* were sectioned at the mid-trunk level (at the level of the black bar in Fig. 2C). We found that *spry3* is expressed in two ventral and two dorsal domains in the spinal cord (Fig. 2D). The ventral expression domain overlaps with that of *hb9* (a motoneuron marker) (Saha et al., 1997), whereas the dorsal expression domain overlaps with that of *hox11L2* (a sensory neuron marker) (Patterson and Krieg, 1999), showing that *spry3* is expressed in spinal motor and sensory neurons (Fig. 2D).

Altogether, these data show that *spry3* has a pattern of expression that is distinct from that of the other *spry* family members, suggesting that it has a specific role during neural development.

Role of Spry3 during neuronal development

Having established that *spry3* is expressed in neuronal cells during embryogenesis, we next examined its function using a morpholino-based knockdown approach. We designed two morpholinos that target the splice donor and splice acceptor site of the unique intron in *spry3*, and their efficacy was assessed by RT-PCR (see Fig. S1A in the supplementary material). The best knockdown was observed using a combination of MO e1i1 and MO i1e2 (referred to hereafter as MOS3). Because *spry3* is expressed specifically in neuronal cells, we tested whether Spry3 plays a role in motor axon development. We compared the organisation of the motor axonal tracts in control and Spry3 morphant embryos, using an antibody directed against acetylated α-tubulin, which specifically recognises differentiated neurons and ciliated cells. Confocal imaging of the whole-mount morphant embryos showed that the axonal tracts of the motoneurons were disorganised when Spry3 expression was knocked down from stage 28 (early tadpole) to stage 40 (Fig. 3A; see Fig. S1B in the supplementary material). To exclude a possible defect in muscle formation, we stained control embryos and Spry3 morphant embryos with a muscle-specific antibody (12-101). We could not detect any difference between control morpholino (MOC)- and MOS3-injected embryos (data not shown). We also quantified the number of differentiating neurons in embryos injected with MOC and MOS3 using an anti-Myt1 (Myelin transcription factor 1) antibody and did not observe any difference (data not shown).

To understand why the axonal tracts were disorganised, embryos stained with acetylated α-tubulin antibody were sectioned and imaged using confocal microscopy (Fig. 3A, lower panels). The axonal tracts were then reconstituted using the Imaris software and the number of branch points was quantified in each sample. The loss of Spry3 function increased axonal branching by 35% (P=0.004, Fig. 3B).

To further characterise the phenotype caused by Spry3 loss of function, we labelled single motoneurons from control embryos and MOS3 embryos (Fig. 3C). We injected MOC and MOS3 at the 1-cell stage and then injected a plasmid that drives the expression of a fusion of Tau (which binds to microtubules) with GFP from the NBT promoter (NBT-τGFP) (Bronchain et al., 1999) in the D1.2 blastomere at the 16-cell stage. The embryos were fixed and stained with an anti-GFP antibody and single neurons imaged by confocal microscopy. As previously shown by staining of the whole motor axonal tract, single MOS3 neurons displayed more branches (neurons per 100 μm of axon: 5.6 for control versus 9 for MOS3; P=0.02). We also quantified the total length of neurons and found that MOS3 neurons are shorter than control neurons (143 μm compared with 105 μm; P=0.009).

spry3 expression depends on BDNF-TrkB

Spry family members are often involved in a negative-feedback loop, i.e. their expression is dependent on the signalling pathway that they regulate (Kim and Bar-Sagi, 2004). Indeed, *spry1*, *spry2* and *spry4* have all been shown to be negative regulators of FGF

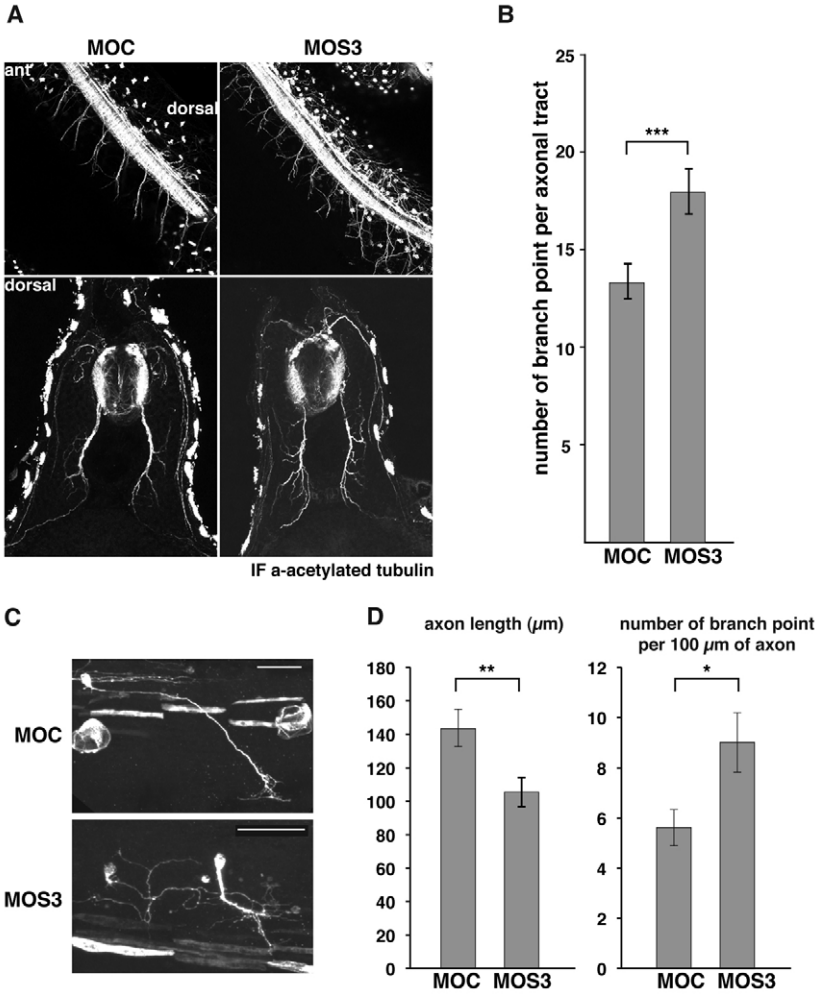

Fig. 3. Spry3 regulates axonal branching. (**A**) Whole-mounts (upper panels) and spinal cord sections (lower panels) of control (MOC) or *spry3* (MOS3) morpholino-injected *Xenopus* embryos stained with anti-acetylated α-tubulin antibodies. For whole-mount, anterior is up, dorsal is right. For sections, dorsal is up. (**B**) Quantification of number of branch points per axonal tract of motoneurons, derived from the analysis of the sections shown in A. Data are expressed as the mean ± s.e.m. of three independent experiments (n=13 embryos for each condition). (**C**) Whole-mount staining of a single motoneuron expressing GFP from MOC and MOS3 embryos. Scale bars: 50 μm. (**D**) Quantification of axon length (left) and number of branch points per 100 μm of axon (right). The data are expressed as the mean ± s.e.m. of three independent experiments (n=19 neurons for MOC and n=24 neurons for MOS3). In all cases, statistical significance was determined using an unpaired Student's t-test; *P=0.02, **P=0.009, ***P=0.004.

signalling during embryogenesis (Furthauer et al., 2001; Komisarczuk et al., 2008; Sivak et al., 2005; Taniguchi et al., 2007), and their pattern of expression is similar to that of *fgf8* (see Fig. S2A in the supplementary material). Furthermore, downregulation of FGF signalling with the FGFR inhibitor SU5402 inhibits *spry1*, *spry2* and *spry4*, but not *spry3*, expression (see Fig. S2B in the supplementary material). This suggests that *spry3* might be involved in the regulation of another signalling pathway.

We observed that *spry3* belongs to a synexpression group comprising *bdnf* and *trkb* (Fig. 4A) (Islam et al., 1996). We therefore tested whether *spry3* expression is dependent on BDNF-TrkB signalling. We knocked down BDNF and TrkB expression using antisense morpholinos and isolated total RNA from whole embryos or dissected neural tubes at stage 26. We then assessed *spry3* expression using real-time PCR. We observed a strong reduction of *spry3* expression, both in whole *Xenopus* embryos and in isolated neural tubes (Fig. 4B). This indicates that *spry3* expression is indeed dependent on BDNF-TrkB signalling. We confirmed these results by knocking down BDNF or TrkB expression using antisense morpholinos and performing in situ hybridisation for *spry3* (Fig. 4C). *spry3* expression was reduced in 74% of BDNF morphants (n=27) and in 83.3% of TrkB morphants (n=24).

Altogether, these data show that *spry3* expression depends on BDNF-TrkB but not FGF, suggesting that Spry3 might regulate BDNF signalling.

Spry3 reduces Erk activation and inhibits calcium signalling downstream of BDNF-TrkB

To establish whether Spry3 is a negative regulator of TrkB signalling, we investigated whether Spry3 affects TrkB-dependent activation of intracellular signalling pathways. TrkB is a tyrosine kinase-type receptor and can activate multiple intracellular signalling pathways, including the Erk, PI3K-Akt and PLCγ-Ca^{2+} pathways (Segal, 2003). To determine whether Spry3 is able to regulate the Erk pathway downstream of TrkB, we injected mRNA encoding TrkB together with GFP, Spry2, Spry3 or Spred1 into fertilised eggs. At blastula stage (stage 8), we dissected the animal cap and stimulated the cells with recombinant BDNF. When animal cap cells express TrkB, BDNF treatment induces a very strong activation of Erk as detected by an anti-pErk antibody (Fig. 5A). This activation was completely abolished when Spred1 was co-expressed, but only reduced in the presence of Spry2 or Spry3. This was despite the fact that Spry2 and Spry3 were expressed at higher levels than Spred1 (Fig. 5A, lower panel). Therefore, Spry3 is only a weak inhibitor of Erk downstream of BDNF-TrkB signalling.

To address whether Spry3 could prevent calcium release downstream of TrkB, we used an oocyte-based calcium assay (Nutt et al., 2001). *Xenopus* oocytes were injected with mRNA encoding TrkB together with GFP, Spry2 or Spry3. Two days later, the oocytes were loaded with $^{45}Ca^{2+}$, washed and then stimulated with

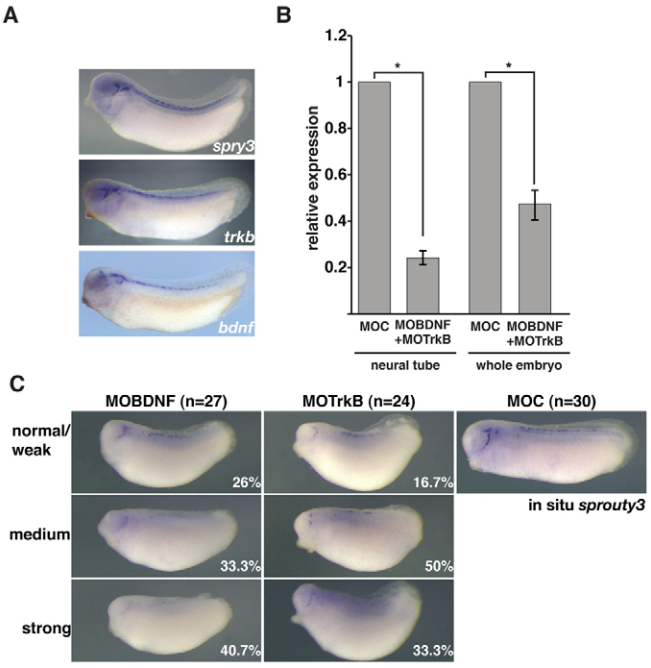

Fig. 4. *spry3* expression is dependent on BDNF-TrkB.
(**A**) Synexpression group of *spry3*. The pattern of expression of *spry3* resembles that of *bdnf* and *trkb*. (**B**) Total RNA from whole embryos or isolated neural tube (stage 26) was purified from *Xenopus* embryos injected with morpholinos against *bdnf* (MO BDNF) or *trkb* (MO TrkB) or with a control morpholino (MOC). *spry3* expression was assessed by real-time PCR using *rpl8* as a reference. Knocking down *bdnf* and *trkb* results in a significant decrease in *spry3* expression (*P<0.005, using a statistical ANOVA test). Error bars indicate mean ± s.e.m. (**C**) *Xenopus* embryos were injected at the 1-cell stage with MO BDNF, MO TrkB or MOC, fixed at stage 28 and processed for whole-mount in situ hybridisation using a probe specific for *spry3*. Embryos are scored as normal/weak when *spry3* expression is detected both in the trigeminal nerve and the spinal cord, as medium when *spry3* expression is only partially detected in the spinal cord and as strong when no expression of *spry3* is detected. The percentage of affected embryos is indicated in each case.

recombinant BDNF. In oocytes expressing TrkB and GFP, this resulted in the rapid release of calcium from intracellular stores to the extracellular medium (Fig. 5B). However, co-expression of either Spry2 or Spry3 caused a complete inhibition of calcium release, indicating that Spry can efficiently inhibit calcium signalling downstream of TrkB. Furthermore, the TrkB-dependent calcium release requires PLCγ activity, as release was blocked with the PLCγ inhibitor U73122 (see Fig. S3 in the supplementary material) (Sato et al., 2000), suggesting that Spry3 inhibits PLCγ-dependent calcium release.

Because TrkB does not induce activation of Akt in animal caps (data not shown), we tested whether Spry3 affects the Akt pathway using transient transfection of HeLa cells (Fig. 4C). HeLa cells were transfected with GFP, Spry3, TrkB plus GFP, or TrkB plus Spry3. BDNF treatment of GFP- or Spry3-expressing cells did not result in Erk or Akt activation. However, TrkB-expressing cells activated both Erk and Akt after 5 minutes of BDNF stimulation. Co-expression of Spry3 together with TrkB did not alter the activation of Erk and Akt, indicating that Spry3 does not inhibit these intracellular signalling pathways (Fig. 5C).

These results show that Spry3 is a weak inhibitor of Erk signalling in *Xenopus* embryonic cells but does not inhibit Erk or Akt signalling downstream of TrkB in HeLa cells. However, Spry3 efficiently prevents calcium release downstream of TrkB signalling.

Spry3 regulates BDNF-induced filopodia in spinal cord neurons

The data described above show that Spry3 inhibits axonal branching in motoneurons in vivo and inhibits calcium release downstream of BDNF-TrkB signalling. To test whether Spry3 regulates axonal morphogenesis downstream of BDNF, we employed spinal cord neurons in culture. It has been shown previously that BDNF-TrkB signalling induces an increase in lamellipodia/filopodia activity in *Xenopus* spinal cord neurons in culture (Gibney and Zheng, 2003; Ming et al., 1997). Therefore, we tested whether Spry3 acts downstream of the BDNF-TrkB pathway by measuring the filopodia/lamellipodia activity of spinal cord neurons when Spry3 expression is knocked down.

Neural tubes of embryos injected with MOC or MOS3 were dissected, dissociated and plated as previously described (Gomez et al., 2003). After 24 hours in culture, neurons were live imaged using DIC time-lapse microscopy, for 20 minutes before and 30 minutes after BDNF stimulation (Fig. 6A; see Movies 1 and 2 in the supplementary material). As previously reported, we observed an increased number of filopodia in the control neurons after BDNF treatment (from 6.4±0.17 to 7.8±0.36 per 100 μm axon length; P=0.01; Fig. 6B) (Ming et al., 1997). Surprisingly, neurons from MOS3 experimental embryos displayed a higher number of filopodia even before BDNF treatment (8.8±0.18, P=0.001), corresponding to an increase of 27% in the number of filopodia compared with control neurons. This could be due to autocrine or paracrine BDNF signalling, as *bdnf*, *trkb* and *spry3* are all expressed in spinal cord cultures (see Fig. S4 in the supplementary material). In the absence of Spry3, BDNF treatment induced only a modest increase in the number of filopodia (9.7±0.11, P=0.004). In effect, BDNF stimulation gave an 18% increase in the number of filopodia in control neurons and this was reduced to a 10% increase when Spry3 was knocked down.

This result suggests that Spry3 inhibits the formation of filopodia in spinal cord neurons. To address whether this is due to negative regulation of BDNF signalling, we performed an epistatic experiment in which we inhibited TrkB activation using a chemical inhibitor (K252a) and asked whether the presence or absence of Spry3 affects filopodia formation (Fig. 6C). We counted the number of new filopodia appearing each minute for 15 minutes before and after K252a treatment. In the absence of K252a, there was a significant difference in the number of new filopodia between control and MOS3 axons (new filopodia per 100 μm of axon: 0.91 in the control versus 1.41 in MOS3; P=0.04). Treatment of axons with K252a reduced the number of new filopodia in both cases (from 0.91 to 0.41 in control, P=0.006; and from 1.41 to 0.57 in MOS3 neurons, P=0.001). However, the difference between control and MOS3 axons treated with K252a is not significant (0.41 in control and 0.57 in MOS3, P=0.41). These results indicate that the excess of filopodia observed in MOS3 axons is dependent on BDNF-TrkB signalling.

Spry3 regulates axon branch formation in mouse cortical neurons

The previous experiments show that loss of function of Spry3 increases filopodia formation in axons. To determine whether the converse was also true, we transfected mouse cortical neurons in

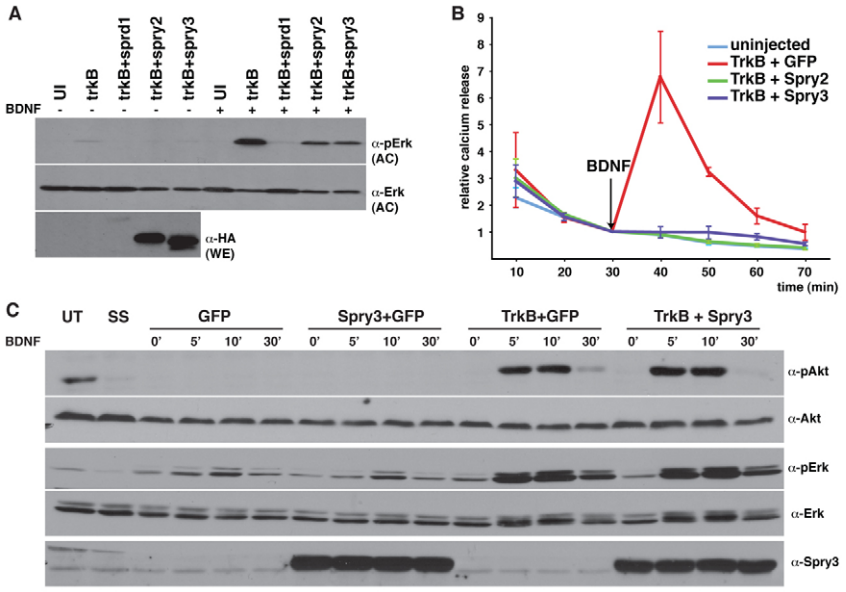

Fig. 5. Biochemical activity of Spry3. (**A**) Spry3 is a weak inhibitor of Erk downstream of BDNF-TrkB signalling. *Xenopus* embryos at 1-cell stage were injected with mRNAs encoding the indicated constructs. At stage 8, animal caps were dissected and stimulated (+) or otherwise (–) with BDNF and the state of phosphorylation of Erk was analysed by western blot using an anti-phospho-Erk antibody (α-pErk). The total amount of Erk was determined using pan-Erk antibodies (α-Erk). Expression of Spred1, Spry2 and Spry3 was confirmed using an anti-HA antibody (bottom panel). UI, uninjected; AC, animal cap; WE, whole embryo. (**B**) Spry3 is a strong inhibitor of calcium signalling downstream of BDNF-TrkB. Oocytes were injected with the indicated constructs and incubated at 16°C for 48 hours. The oocytes were then loaded with $^{45}Ca^{2+}$ and then stimulated with BDNF, resulting in a peak of calcium release in the control conditions but not when Spry2 or Spry3 is expressed. Error bars indicate mean ± s.e.m. (**C**) Spry3 does not inhibit Erk and Akt signalling in HeLa cells. HeLa cells were transfected with the indicated constructs and 36 hours later were stimulated with BDNF for the indicated time (minutes). Total protein was subsequently analysed by western blot using anti-phospho-Akt (α-pAkt), anti-pan Akt (α-Akt), anti-phospho-Erk and anti-pan Erk antibodies. Expression of Spry3 was confirmed using an anti-Spry3 antibody. UT, untransfected; SS, serum starved.

culture with GFP alone (control) or together with Spry3 (Fig. 7A). As mouse cortical neurons do not express endogenous *Spry3* (data not shown), this allowed us to test its role in BDNF-induced axonal branching. Spry3 overexpression significantly increased the percentage of neurons with no axon branching, as well as reducing the percentage of neurons with more than four branches (Fig. 7B). Importantly, we quantified the mean length of the axons as previously described (Dajas-Bailador et al., 2008) and did not detect any difference upon overexpression of Spry3 (Fig. 7C).

We also tested whether Spry3 could regulate BDNF-induced branching in this system (Fig. 7D). Treatment of mouse cortical neurons with BDNF increased the proportion of neurons with more than five branches (from 10% to 25%, Fig. 7D). However, this effect was reversed by the expression of Spry3, indicating that Spry3 can prevent BDNF-induced branches. These data show that Spry3 regulates axon branching and indicate that this function might be conserved in mammals.

Altogether, our results show that Spry3 inhibits branching of motoneurons in vivo and the ability of BDNF-TrkB to induce filopodia in neurons in culture. Together with our biochemical data showing that Spry3 inhibits calcium release downstream of TrkB signalling, we propose a model whereby BDNF induces filopodia and branching in a calcium-dependent manner that can be inhibited by Spry3 (Fig. 8).

DISCUSSION

Spry family members have been shown to play a crucial role in branching morphogenesis in a variety of organs and systems, including the kidney, lung and vascular system (Horowitz and Simons, 2008). Here, the function of Spry3 during development is reported for the first time. We found that Spry3 is expressed in the trigeminal nerve, as well as in spinal motor and sensory neurons. Furthermore, we provide evidence that *spry3* is a BDNF-TrkB-dependent gene. At the molecular level, Spry3 reduces Erk activation and inhibits calcium signalling in response to TrkB activation. We also found that Spry3 regulates axon branching in vivo and prevents BDNF-induced filopodia formation in spinal neurons in culture. Hence, we propose that Spry3 acts downstream of BDNF-TrkB in a negative-feedback loop to regulate axon branching in spinal motoneurons by inhibiting calcium signalling.

Regulation of branching morphogenesis by Spry proteins

Inactivation of Spry function leads to defects in branching morphogenesis in a variety of organisms and organs (Horowitz and Simons, 2008). Despite all the data reported on Spry function, the molecular mechanisms by which Spry family members regulate branching are still unclear. In mammalian tissue culture systems, Spry proteins have been shown to inhibit Erk activation downstream of a plethora of growth factors, including FGF, VEGF-A, BDNF and GDNF (Cabrita and Christofori, 2008; Gross et al., 2007; Impagnatiello et al., 2001; Ishida et al., 2007; Taniguchi et al., 2009a). In *Xenopus* embryos, we have shown that Spry1 and Spry2 inhibit the Ca^{2+} pathway downstream of FGF (Nutt et al., 2001; Sivak et al., 2005). Furthermore, Spry4 inhibits Ca^{2+} release and activation of PKC-dependent pathways downstream of VEGF-A in human embryonic kidney cells. Interestingly, Spry4 inhibits activation of Erk downstream of VEGF-A, which is PKC

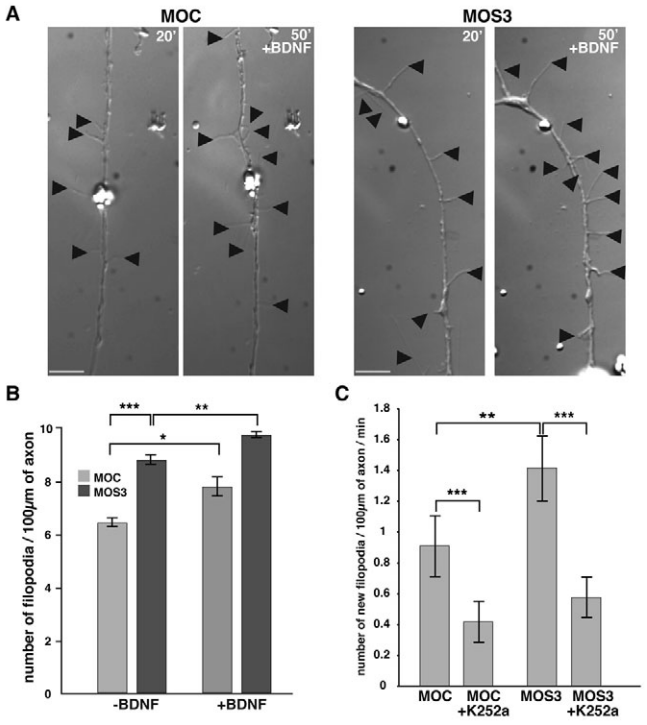

Fig. 6. Spry3 represses the filopodial activity of spinal cord neurons. (**A**) Loss of Spry3 function leads to an increase in the number of filopodia. DIC images of spinal cord neurons from control (MOC) and Spry3 morphant (MOS3) *Xenopus* embryos before (left of each pair) and after (right) stimulation with BDNF. Arrowheads indicate filopodia. (**B**) Quantification of the number of filopodia per 100 μm of axon. The total number of filopodia was counted each minute and the graph represents the mean of the mean±s.e.m. of each axon before (–BDNF) and after BNDF treatment (+BDNF), when Spry3 expression is downregulated (MOS3, *n*=16) or in control (MOC, *n*=16) from three independent experiments. (**C**) Spry3 represses TrkB-induced filopodia. Neurons from MOC and MOS3 embryos were imaged 15 minutes before and 15 minutes after treatment with the TrkB inhibitor K252a. The number of new filopodia was determined by comparison with the preceding frame. The number of new filopodia per 100 μm of axon per minute is shown. MOC, *n*=20; MOS3, *n*=22; mean ± s.e.m. from three independent experiments. In B and C, statistical significance was determined using a two-tailed Student's *t*-test (paired when comparing the same neurons before and after treatment, unpaired when comparing different population of neurons); **P*=0.01, ***P*=0.04, ****P*=0.001.

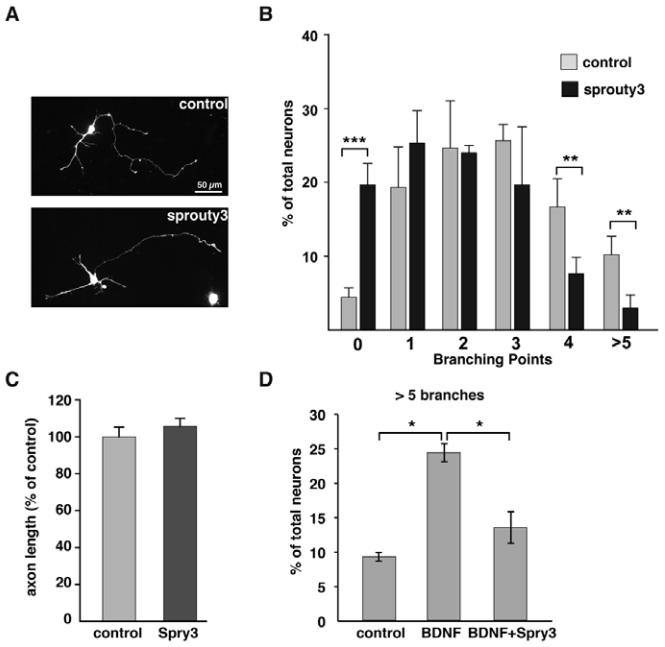

Fig. 7. Spry3 regulates axonal branching in mouse cortical neurons. (**A**) Effect of Spry3 overexpression in mouse cortical neurons. Cortical neurons were isolated from E16 mouse embryos and transfected with GFP alone (top) or together with Spry3 (bottom). (**B**) GFP-positive neurons were then imaged by microscopy and the number of branch points was determined by quantifying the number of neurons with 'x' branch points in control cortical neurons and in cortical neurons overexpressing Spry3. Data are expressed (mean ± s.e.m.) as a percentage of total neurons from three independent experiments (*n*=117 for axons transfected with GFP and *n*=84 for axons also transfected with Spry3). (**C**) The axon length of the same neurons as in A was measured and found to be unaffected by Spry3 overexpression. (**D**) GFP-positive neurons as in B were treated or otherwise with BDNF. Shown is the percentage of neurons (mean ± s.e.m.) with five or more branches from three independent experiments (*n*=129 for control, *n*=114 for BDNF treated and *n*=87 for BDNF+Spry). In B and C, statistical significance was determined using a paired Student's *t*-test; **P*=0.05, ***P*=0.01, ****P*=0.001.

dependent, but not downstream of VEGF-C, which is Ras dependent (Ayada et al., 2009). This suggests that Spry4 most likely acts via the PLCγ-Ca^{++} and not the Ras pathway, leading to both inhibition of Ca^{2+} mobilisation and inhibition of Erk activation via PKC. It has also recently been shown that murine Spry1 and Spry2 can bind PLCγ thereby inhibiting the production of IP3 and calcium release in NIH3T3 cells, and that they regulate PLCγ activity in T cells (Akbulut et al., 2010). Together with our data, these studies suggest that regulation of the PLCγ-Ca^{2+} pathway by Spry proteins plays important roles in various biological contexts.

Spry3 is present in all vertebrate genomes analysed so far, but nothing has been reported on its function. Here, we show for the first time that Spry3 knockdown increases branching in peripheral motor axons in vivo and increases lamellipodia/filopodia activity in *Xenopus* spinal cord cultures. At the molecular level, we show that Spry3 inhibits the Ca^{2+} pathway in response to BDNF. Furthermore, we found that Spry3 reduces Erk activation downstream of BDNF, although its inhibitory action is not as strong as that of Spred1. Whether the reduction in activated Erk we observed in the presence of Spry3 is due to the inhibition of PLCγ (as is the case for Spry4 downstream of VEGF-A) or reflects direct inhibition of the Erk pathway is not known. Importantly, Spry3 does not inhibit Erk activation in a mammalian cell line, showing that this result is not a peculiarity of *Xenopus* cells.

Intrinsic versus extrinsic regulation of axonal branching

Although there are numerous studies supporting a role for extrinsic factors in axon branching (Campbell et al., 2001; Feldner et al., 2007; Marler et al., 2008; Morita et al., 2006; Tang et al., 2004), the intracellular components that regulate axon branching remain poorly understood.

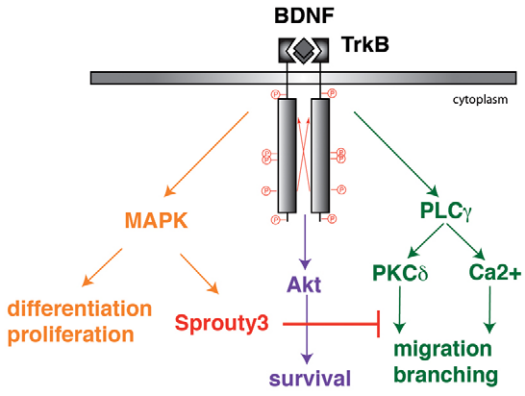

Fig. 8. Model of the role of Spry3 in motoneurons. BDNF-TrkB signalling induces *spry3* expression possibly via MAPK. Spry3 then inhibits specifically PLCγ-Ca^{2+}, thereby preventing premature or excess axonal branching. BDNF-TrkB signalling induces *spry3* expression, possibly via MAPK. Spry3 then inhibits specifically PLCγ-Ca^{2+}, thereby preventing premature or excess axonal branching.

In cultured hippocampal neurons, BDNF can induce neurite outgrowth by inhibiting the protease Calpain. The inhibition of Calpain presumably stabilises Cortactin, which is necessary for the initial sprouting of filopodia (Mingorance-Le Meur and O'Connor, 2009). Although Calpain is known to be regulated by calcium, in hippocampal neurons it has been shown to be inhibited by PKA downstream of BDNF (Mingorance-Le Meur and O'Connor, 2009). Interestingly, Calpain is also expressed in the *Xenopus* spinal cord and its activity is regulated by calcium transients (Robles et al., 2003). It has also recently been shown that Nedd4, an E3 ubiquitin ligase, is necessary to turn off PTEN, causing an increase in PI3K signalling and inducing axon branching in *Xenopus* retinal ganglion cells (Drinjakovic et al., 2010). In a concomitant paper, the knockout of *Nedd4-1* in mice showed that Nedd4 is necessary for dendrite arborisation and neurite growth (Kawabe et al., 2010). Together, these papers reveal a new intracellular pathway involving ubiquitylation of specific proteins to control neurite outgrowth. How the activity of Nedd4 is regulated remains unclear.

Here, we have identified a new signalling regulator, Spry3, as an intrinsic factor that controls axon branching. Since Spry3 inhibits Ca^{2+} release, it is likely that Spry3 inhibits axon branching by inhibiting calcium signalling. In support of this hypothesis it has been shown that Netrin1 promotes axon branching by inducing repetitive high-frequency Ca^{2+} transients, which occur locally in axonal regions and coincide spatially with the formation of new filopodia that develop into branches. Importantly, these Ca^{2+} transients are necessary for the elaboration of branches in response to Netrin1 (Tang and Kalil, 2005). Moreover, in *Xenopus* retinal ganglion cells that arborise in the optic tectum, new axon branches arise from sites with locally increased intracellular Ca^{2+} concentration (Edwards and Cline, 1999). Additional reports show that increased intracellular Ca^{2+} concentration induces the projection of filopodia from both growth cones (Davenport and Kater, 1992) and axons (Lau et al., 1999), consistent with our finding that Spry3 knockdown increases the number of filopodia projecting from the axon shaft. Therefore, our data showing that Spry3 inhibits Ca^{2+} release in oocytes are consistent with the role attributed to calcium signalling in the induction of filopodia and axon branching.

Role of BDNF-TrkB signalling in motoneurons

In mouse, *Trkb* (*Ntrk2*) and its ligands *Bdnf* and *NT4* (*Ntf5*) are all expressed in motoneurons (Henderson et al., 1993). Furthermore, BDNF and NT4 have been shown to promote the survival of rat embryonic motoneurons in culture (Henderson et al., 1993) and BDNF can also promote the formation of neuromuscular synapses (Lohof et al., 1993). However, *Trkb* knockout results only in a reduction of motoneurons (~35%) and *Bdnf*$^{-/-}$ mice do not exhibit a loss of motoneurons (Ernfors et al., 1994; Jones et al., 1994; Klein et al., 1993; Snider, 1994), suggesting a role for BDNF-TrkB signalling other than in survival. Interestingly, BDNF has been shown to be important for the survival of sensory neurons and the trigeminal nerve in mouse (Liu and Jaenisch, 2000), cell types that also express *spry3* in *Xenopus*. The role of Spry3 in other neuronal populations will need to be elucidated in the future.

In *Xenopus*, knockdown of BDNF expression using morpholinos causes a complete loss of motor axon extension from the spinal cord (K.D., Jeff K. Huang and E.A., unpublished), suggesting that BDNF-TrkB signalling is required for the normal development of motoneurons in *Xenopus*. It is also known that BDNF induces an increase in filopodia/lamellipodia activity in spinal cord neurons in culture (Gibney and Zheng, 2003; Ming et al., 1997). In vivo, motoneurons need to extend their axons a considerable distance before starting to innervate their target organs. Although extrinsic clues have been shown to play a role in preventing early branching of motoneurons (Feldner et al., 2007), we show here that a target gene of BDNF-TrkB signalling, Spry3, is also important. How *spry3* expression is regulated is unknown, but our data indicate that neurons will respond differently to BDNF depending on whether or not they express Spry3. Interestingly, it has recently been shown that gradual and acute stimulation of neurons with BDNF lead to the expression of different genes (Ji et al., 2010). Whether *spry3* expression is regulated in a dose-dependent manner will require further investigation.

In conclusion, we have shown that Spry3 inhibits axon branching in vivo and negatively regulates signalling downstream of BDNF-TrkB. Furthermore, Spry3 prevents the induction of BDNF-induced filopodia in spinal cord neurons and BDNF-induced branching in cortical neurons in culture. Because calcium signalling has been shown to induce branching, and Spry3 inhibits calcium release downstream of BDNF-TrkB signalling, we propose that Spry3 is turned on by BDNF in a feedback loop to repress calcium signalling and hence branching, thereby fine-tuning RTK signalling and avoiding excessive axon branch formation. It will be interesting to investigate whether this mechanism is also present in branched multicellular organs.

Acknowledgements
We thank Peter March for help with the time-lapse microscopy. This work was supported by a Wellcome Trust 4-year PhD studentship to N. Panagiotaki, an MRC project grant to F.D.-B. and N. Papalopulu, a Wellcome Trust Senior Research Fellowship to N. Papalopulu, a Wellcome Trust Programme Grant to E.A. and an RCUK fellowship to K.D. Deposited in PMC for release after 6 months.

Competing interests statement
The authors declare no competing financial interests.

Supplementary material
Supplementary material for this article is available at
http://dev.biologists.org/lookup/suppl/doi:10.1242/dev.053173/-/DC1

References

Acebes, A. and Ferrus, A. (2000). Cellular and molecular features of axon collaterals and dendrites. *Trends Neurosci.* **23**, 557-565.

Akbulut, S., Reddi, A. L., Aggarwal, P., Ambardekar, C., Canciani, B., Kim, M. K. H., Hix, L., Vilimas, T., Mason, J., Basson, M. A. et al. (2010). Sprouty proteins inhibit receptor-mediated activation of phosphatidylinositol-specific phospholipase C. *Mol. Biol. Cell* **21**, 3487-3496.
Ayada, T., Taniguchi, K., Okamoto, F., Kato, R., Komune, S., Takaesu, G. and Yoshimura, A. (2009). Sprouty4 negatively regulates protein kinase C activation by inhibiting phosphatidylinositol 4,5-biphosphate hydrolysis. *Oncogene* **28**, 1076-1088.
Barde, Y. A., Edgar, D. and Thoenen, H. (1982). Purification of a new neurotrophic factor from mammalian brain. *EMBO J.* **1**, 549-553.
Basson, M. A., Akbulut, S., Watson-Johnson, J., Simon, R., Carroll, T. J., Shakya, R., Gross, I., Martin, G. R., Lufkin, T., McMahon, A. P. et al. (2005). Sprouty1 is a critical regulator of GDNF/RET-mediated kidney induction. *Dev. Cell* **8**, 229-239.
Basson, M. A., Watson-Johnson, J., Shakya, R., Akbulut, S., Hyink, D., Costantini, F. D., Wilson, P. D., Mason, I. J. and Licht, J. D. (2006). Branching morphogenesis of the ureteric epithelium during kidney development is coordinated by the opposing functions of GDNF and Sprouty1. *Dev. Biol.* **299**, 466-477.
Bronchain, O. J., Hartley, K. O. and Amaya, E. (1999). A gene trap approach in Xenopus. *Curr. Biol.* **9**, 1195-1198.
Cabrita, M. A. and Christofori, G. (2008). Sprouty proteins, masterminds of receptor tyrosine kinase signaling. *Angiogenesis* **11**, 53-62.
Campbell, D. S., Regan, A. G., Lopez, J. S., Tannahill, D., Harris, W. A. and Holt, C. E. (2001). Semaphorin 3A elicits stage-dependent collapse, turning, and branching in Xenopus retinal growth cones. *J. Neurosci.* **21**, 8538-8547.
Chen, Y., Costa, R. M., Love, N. R., Soto, X., Roth, M., Paredes, R. and Amaya, E. (2009). C/EBPalpha initiates primitive myelopoiesis in pluripotent embryonic cells. *Blood* **114**, 40-48.
Cohen-Cory, S. and Fraser, S. E. (1995). Effects of brain-derived neurotrophic factor on optic axon branching and remodelling in vivo. *Nature* **378**, 192-196.
Costa, R. M., Soto, X., Chen, Y., Zorn, A. M. and Amaya, E. (2008). spib is required for primitive myeloid development in Xenopus. *Blood* **112**, 2287-2296.
Cunningham, M. E. and Greene, L. A. (1998). A function-structure model for NGF-activated TRK. *EMBO J.* **17**, 7282-7293.
Dajas-Bailador, F., Jones, E. V. and Whitmarsh, A. J. (2008). The JIP1 scaffold protein regulates axonal development in cortical neurons. *Curr. Biol.* **18**, 221-226.
Davenport, R. W. and Kater, S. B. (1992). Local increases in intracellular calcium elicit local filopodial responses in Helisoma neuronal growth cones. *Neuron* **9**, 405-416.
Drinjakovic, J., Jung, H., Campbell, D. S., Strochlic, L., Dwivedy, A. and Holt, C. E. (2010). E3 Ligase Nedd4 Promotes Axon Branching by Downregulating PTEN. *Neuron* **65**, 341-357.
Edwards, J. A. and Cline, H. T. (1999). Light-induced calcium influx into retinal axons is regulated by presynaptic nicotinic acetylcholine receptor activity in vivo. *J. Neurophysiol.* **81**, 895-907.
Ernfors, P., Lee, K. F. and Jaenisch, R. (1994). Mice lacking brain-derived neurotrophic factor develop with sensory deficits. *Nature* **368**, 147-150.
Feldner, J., Reimer, M. M., Schweitzer, J., Wendik, B., Meyer, D., Becker, T. and Becker, C. G. (2007). PlexinA3 restricts spinal exit points and branching of trunk motor nerves in embryonic zebrafish. *J. Neurosci.* **27**, 4978-4983.
Furthauer, M., Reifers, F., Brand, M., Thisse, B. and Thisse, C. (2001). sprouty4 acts in vivo as a feedback-induced antagonist of FGF signaling in zebrafish. *Development* **128**, 2175-2186.
Gibney, J. and Zheng, J. Q. (2003). Cytoskeletal dynamics underlying collateral membrane protrusions induced by neurotrophins in cultured Xenopus embryonic neurons. *J. Neurobiol.* **54**, 393-405.
Goldberg, J. L. (2004). Intrinsic neuronal regulation of axon and dendrite growth. *Curr. Opin. Neurobiol.* **14**, 551-557.
Gomez, T. M., Harrigan, D., Henley, J. and Robles, E. (2003). Working with Xenopus spinal neurons in live cell culture. *Methods Cell Biol.* **71**, 129-156.
Gross, I., Armant, O., Benosman, S., de Aguilar, J. L., Freund, J. N., Kedinger, M., Licht, J. D., Gaiddon, C. and Loeffler, J. P. (2007). Sprouty2 inhibits BDNF-induced signaling and modulates neuronal differentiation and survival. *Cell Death Differ.* **14**, 1802-1812.
Hacohen, N., Kramer, S., Sutherland, D., Hiromi, Y. and Krasnow, M. A. (1998). sprouty encodes a novel antagonist of FGF signaling that patterns apical branching of the Drosophila airways. *Cell* **92**, 253-263.
Hanafusa, H., Torii, S., Yasunaga, T. and Nishida, E. (2002). Sprouty1 and Sprouty2 provide a control mechanism for the Ras/MAPK signalling pathway. *Nat. Cell Biol.* **4**, 850-858.
Harland, R. M. (1991). In situ hybridization: an improved whole-mount method for Xenopus embryos. *Methods Cell Biol.* **36**, 685-695.
Heasman, J., Kofron, M. and Wylie, C. (2000). Beta-catenin signaling activity dissected in the early Xenopus embryo: a novel antisense approach. *Dev. Biol.* **222**, 124-134.
Henderson, C. E., Camu, W., Mettling, C., Gouin, A., Poulsen, K., Karihaloo, M., Rullamas, J., Evans, T., McMahon, S. B., Armanini, M. P. et al. (1993). Neurotrophins promote motor neuron survival and are present in embryonic limb bud. *Nature* **363**, 266-270.
Horowitz, A. and Simons, M. (2008). Branching morphogenesis. *Circ. Res.* **103**, 784-795.
Huang, E. J. and Reichardt, L. F. (2001). Neurotrophins: roles in neuronal development and function. *Annu. Rev. Neurosci.* **24**, 677-736.
Huang, J. K., Dorey, K., Ishibashi, S. and Amaya, E. (2007). BDNF promotes target innervation of Xenopus mandibular trigeminal axons in vivo. *BMC Dev. Biol.* **7**, 59.
Impagnatiello, M. A., Weitzer, S., Gannon, G., Compagni, A., Cotten, M. and Christofori, G. (2001). Mammalian sprouty-1 and -2 are membrane-anchored phosphoprotein inhibitors of growth factor signaling in endothelial cells. *J. Cell Biol.* **152**, 1087-1098.
Ishida, M., Ichihara, M., Mii, S., Jijiwa, M., Asai, N., Enomoto, A., Kato, T., Majima, A., Ping, J., Murakumo, Y. et al. (2007). Sprouty2 regulates growth and differentiation of human neuroblastoma cells through RET tyrosine kinase. *Cancer Sci.* **98**, 815-821.
Islam, N., Gagnon, F. and Moss, T. (1996). Catalytic and non-catalytic forms of the neurotrophin receptor xTrkB mRNA are expressed in a pseudo-segmental manner within the early Xenopus central nervous system. *Int. J. Dev. Biol.* **40**, 973-983.
Ji, Y., Lu, Y., Yang, F., Shen, W., Tang, T. T., Feng, L., Duan, S. and Lu, B. (2010). Acute and gradual increases in BDNF concentration elicit distinct signaling and functions in neurons. *Nat. Neurosci.* **13**, 302-309.
Jones, K. R., Farinas, I., Backus, C. and Reichardt, L. F. (1994). Targeted disruption of the BDNF gene perturbs brain and sensory neuron development but not motor neuron development. *Cell* **76**, 989-999.
Kawabe, H., Neeb, A., Dimova, K., Young, S. M., Jr, Takeda, M., Katsurabayashi, S., Mitkovski, M., Malakhova, O. A., Zhang, D. E., Umikawa, M. et al. (2010). Regulation of Rap2A by the ubiquitin ligase Nedd4-1 controls neurite development. *Neuron* **65**, 358-372.
Kim, H. J. and Bar-Sagi, D. (2004). Modulation of signalling by Sprouty: a developing story. *Nat. Rev. Mol. Cell Biol.* **5**, 441-450.
Klein, O. D., Minowada, G., Peterkova, R., Kangas, A., Yu, B. D., Lesot, H., Peterka, M., Jernvall, J. and Martin, G. R. (2006). Sprouty genes control diastema tooth development via bidirectional antagonism of epithelial-mesenchymal FGF signaling. *Dev. Cell* **11**, 181-190.
Klein, R., Smeyne, R. J., Wurst, W., Long, L. K., Auerbach, B. A., Joyner, A. L. and Barbacid, M. (1993). Targeted disruption of the trkB neurotrophin receptor gene results in nervous system lesions and neonatal death. *Cell* **75**, 113-122.
Komisarczuk, A. Z., Topp, S., Stigloher, C., Kapsimali, M., Bally-Cuif, L. and Becker, T. S. (2008). Enhancer detection and developmental expression of zebrafish sprouty1, a member of the fgf8 synexpression group. *Dev. Dyn.* **237**, 2594-2603.
Lau, P. M., Zucker, R. S. and Bentley, D. (1999). Induction of filopodia by direct local elevation of intracellular calcium ion concentration. *J. Cell Biol.* **145**, 1265-1275.
Lea, R., Papalopulu, N., Amaya, E. and Dorey, K. (2009). Temporal and spatial expression of FGF ligands and receptors during Xenopus development. *Dev. Dyn.* **238**, 1467-1479.
Liu, X. and Jaenisch, R. (2000). Severe peripheral sensory neuron loss and modest motor neuron reduction in mice with combined deficiency of brain-derived neurotrophic factor, neurotrophin 3 and neurotrophin 4/5. *Dev. Dyn.* **218**, 94-101.
Lohof, A. M., Ip, N. Y. and Poo, M. M. (1993). Potentiation of developing neuromuscular synapses by the neurotrophins NT-3 and BDNF. *Nature* **363**, 350-353.
Marler, K. J., Becker-Barroso, E., Martinez, A., Llovera, M., Wentzel, C., Poopalasundaram, S., Hindges, R., Soriano, E., Comella, J. and Drescher, U. (2008). A TrkB/EphrinA interaction controls retinal axon branching and synaptogenesis. *J. Neurosci.* **28**, 12700-12712.
Mason, J. M., Morrison, D. J., Albert Basson, M. and Licht, J. D. (2006). Sprouty proteins: multifaceted negative-feedback regulators of receptor tyrosine kinase signaling. *Trends Cell Biol.* **16**, 45-54.
Ming, G., Lohof, A. M. and Zheng, J. Q. (1997). Acute morphogenic and chemotropic effects of neurotrophins on cultured embryonic Xenopus spinal neurons. *J. Neurosci.* **17**, 7860-7871.
Ming, G., Song, H., Berninger, B., Inagaki, N., Tessier-Lavigne, M. and Poo, M. (1999). Phospholipase C-gamma and phosphoinositide 3-kinase mediate cytoplasmic signaling in nerve growth cone guidance. *Neuron* **23**, 139-148.
Mingorance-Le Meur, A. and O'Connor, T. P. (2009). Neurite consolidation is an active process requiring constant repression of protrusive activity. *EMBO J.* **28**, 248-260.
Minichiello, L. (2009). TrkB signalling pathways in LTP and learning. *Nat. Rev. Neurosci.* **10**, 850-860.
Morita, A., Yamashita, N., Sasaki, Y., Uchida, Y., Nakajima, O., Nakamura, F., Yagi, T., Taniguchi, M., Usui, H., Katoh-Semba, R. et al. (2006). Regulation of dendritic branching and spine maturation by semaphorin3A-Fyn signaling. *J. Neurosci.* **26**, 2971-2980.

Musci, T. J., Amaya, E. and Kirschner, M. W. (1990). Regulation of the fibroblast growth factor receptor in early Xenopus embryos. *Proc. Natl. Acad. Sci. USA* **87**, 8365-8369.
Navarro, X. (2009). Neural plasticity after nerve injury and regeneration. *Int. Rev. Neurobiol.* **87**, 483-505.
Nutt, S. L., Dingwell, K. S., Holt, C. E. and Amaya, E. (2001). Xenopus Sprouty2 inhibits FGF-mediated gastrulation movements but does not affect mesoderm induction and patterning. *Genes Dev.* **15**, 1152-1166.
O'Donnell, M., Chance, R. K. and Bashaw, G. J. (2009). Axon growth and guidance: receptor regulation and signal transduction. *Annu. Rev. Neurosci.* **32**, 383-412.
Patterson, K. D. and Krieg, P. A. (1999). Hox11-family genes XHox11 and XHox11L2 in xenopus: XHox11L2 expression is restricted to a subset of the primary sensory neurons. *Dev. Dyn.* **214**, 34-43.
Reichardt, L. F. (2006). Neurotrophin-regulated signalling pathways. *Philos. Trans. R. Soc. Lond. B Biol. Sci.* **361**, 1545-1564.
Robles, E., Huttenlocher, A. and Gomez, T. M. (2003). Filopodial calcium transients regulate growth cone motility and guidance through local activation of calpain. *Neuron* **38**, 597-609.
Saha, M. S., Miles, R. R. and Grainger, R. M. (1997). Dorsal-ventral patterning during neural induction in Xenopus: assessment of spinal cord regionalization with xHB9, a marker for the motor neuron region. *Dev. Biol.* **187**, 209-223.
Sasaki, A., Taketomi, T., Wakioka, T., Kato, R. and Yoshimura, A. (2001). Identification of a dominant negative mutant of Sprouty that potentiates fibroblast growth factor- but not epidermal growth factor-induced ERK activation. *J. Biol. Chem.* **276**, 36804-36808.
Sato, K.-i., Tokmakov, A. A., Iwasaki, T. and Fukami, Y. (2000). Tyrosine kinase-dependent activation of phospholipase C[gamma] is required for calcium transient in Xenopus egg fertilization. *Dev. Biol.* **224**, 453-469.
Segal, R. A. (2003). Selectivity in neurotrophin signaling: theme and variations. *Annu. Rev. Neurosci.* **26**, 299-330.
Shim, K., Minowada, G., Coling, D. E. and Martin, G. R. (2005). Sprouty2, a mouse deafness gene, regulates cell fate decisions in the auditory sensory epithelium by antagonizing FGF signaling. *Dev. Cell* **8**, 553-564.
Sivak, J. M., Petersen, L. F. and Amaya, E. (2005). FGF signal interpretation is directed by Sprouty and Spred proteins during mesoderm formation. *Dev. Cell* **8**, 689-701.
Snider, W. D. (1994). Functions of the neurotrophins during nervous system development: what the knockouts are teaching us. *Cell* **77**, 627-638.
Tang, F. and Kalil, K. (2005). Netrin-1 induces axon branching in developing cortical neurons by frequency-dependent calcium signaling pathways. *J. Neurosci.* **25**, 6702-6715.
Tang, X. Q., Tanelian, D. L. and Smith, G. M. (2004). Semaphorin3A inhibits nerve growth factor-induced sprouting of nociceptive afferents in adult rat spinal cord. *J. Neurosci.* **24**, 819-827.
Taniguchi, K., Ayada, T., Ichiyama, K., Kohno, R., Yonemitsu, Y., Minami, Y., Kikuchi, A., Maehara, Y. and Yoshimura, A. (2007). Sprouty2 and Sprouty4 are essential for embryonic morphogenesis and regulation of FGF signaling. *Biochem. Biophys. Res. Commun.* **352**, 896-902.
Taniguchi, K., Ishizaki, T., Ayada, T., Sugiyama, Y., Wakabayashi, Y., Sekiya, T., Nakagawa, R. and Yoshimura, A. (2009a). Sprouty4 deficiency potentiates Ras-independent angiogenic signals and tumor growth. *Cancer Sci.* **100**, 1648-1654.
Taniguchi, K., Sasaki, K., Watari, K., Yasukawa, H., Imaizumi, T., Ayada, T., Okamoto, F., Ishizaki, T., Kato, R., Kohno, R. et al. (2009b). Suppression of Sproutys has a therapeutic effect for a mouse model of ischemia by enhancing angiogenesis. *PLoS ONE* **4**, e5467.
Tefft, J. D., Lee, M., Smith, S., Leinwand, M., Zhao, J., Bringas, P., Jr, Crowe, D. L. and Warburton, D. (1999). Conserved function of mSpry-2, a murine homolog of Drosophila sprouty, which negatively modulates respiratory organogenesis. *Curr. Biol.* **9**, 219-222.
Xu, B., Zang, K., Ruff, N. L., Zhang, Y. A., McConnell, S. K., Stryker, M. P. and Reichardt, L. F. (2000). Cortical degeneration in the absence of neurotrophin signaling: dendritic retraction and neuronal loss after removal of the receptor TrkB. *Neuron* **26**, 233-245.
Yoshii, A. and Constantine-Paton, M. (2010). Postsynaptic BDNF-TrkB signaling in synapse maturation, plasticity, and disease. *Dev. Neurobiol.* **70**, 304-322.